Short-time critical dynamics at perfect and imperfect surfaces

S. Z. Lin[1,2] and B. Zheng[1,*]
[1]*Zhejiang Institute of Modern Physics, Zhejiang University, Hangzhou 310027, China*
[2]*National Institute for Materials Science, Tsukuba 305-0047, Japan*
(Received 20 May 2008; published 30 July 2008)

With Monte Carlo simulations, we study the dynamic relaxation at perfect and imperfect surfaces of the three-dimensional Ising model with an ordered initial state. The time evolution of the surface magnetization, the line magnetization of the defect line, and the corresponding susceptibilities and second cumulants is carefully examined. Universal dynamic scaling forms including a dynamic crossover scaling form are identified at the ordinary, special, and surface phase transitions. The critical exponents β_1 of the surface magnetization and β_2 of the line magnetization are extracted. The impact of the defect line on the universality classes is investigated.

DOI: 10.1103/PhysRevE.78.011127 PACS number(s): 64.60.Ht

I. INTRODUCTION

In the past decades, the critical behaviors of surfaces have been extensively studied, and the phase diagram is well established [1–4]. The surface effect often plays a crucial role in experiments and theories, especially for multilayer systems. Such a topic becomes even more important when nanoscale materials are concerned. In a recent experiment, for example, an anomalous temperature profile of the phase transition was observed in the presence of a ferromagnetic surface [5]. In the literature, most works concentrate on the static critical behaviors [6–11] and the critical dynamics in the long-time regime [12–14], when the dynamic system reaches almost or is already in the equilibrium state. The critical dynamics of a surface in the *macroscopic* short-time regime—i.e., when the dynamic system is still far from equilibrium—has been much less touched.

Meanwhile, the short-time critical dynamics of bulk has been established in the past decade and successfully applied to different physical systems [15–27]. Based on the short-time dynamic scaling form, new techniques for the measurements of both dynamic and static critical exponents as well as the critical temperature have been developed [17,28–32]. Recent progress can be found partially in Refs. [21,23,33–35] and references therein. Naturally, the dynamic relaxation of surface in the short-time regime is also important, and worthwhile for careful studies [4,36]. It is recently reported that in nonequilibrium states, the surface cluster dissolution may take place instead of the domain growth [37,38]. In these works, the dynamic relaxation starting from a *high-temperature* state is concerned. Very recently, it has been observed that the dynamic relaxation around a surface shares certain common features with domain-wall motion [27,35].

Obviously, the physical phenomena are more complicated, when both a surface and an initial state exist. The short-time critical dynamics at a surface needs careful theoretical analysis and numerical simulations. In this paper, with Monte Carlo simulations we systematically investigate the short-time critical dynamics at *perfect and imperfect surfaces*. We extend the universal dynamic scaling form to the dynamic relaxation at surfaces, starting from an *ordered* state. At the *ordinary, special*, and *surface* phase transitions, the dynamic scaling behaviors of the surface magnetization, the line magnetization of the defect line, and the corresponding susceptibilities and second cumulants are identified. Around the special transition, *a dynamic crossover scaling form* is revealed. The static critical exponent β_1 of the surface magnetization and β_2 of the line magnetization of the defect line as well the dynamic exponent z and crossover exponent ϕ are extracted from the dynamic behavior in the macroscopic short-time regime. The impact of the defect line on the universality classes is shown. By the short-time dynamic approach, the surface transition and special transition temperatures can be also detected.

The remaining part of the paper is organized as follows. In Sec. II, the model and scaling analysis are presented. In Secs. III and IV, the dynamic relaxation on perfect and imperfect surfaces is studied. In Sec. V, the results are summarized.

II. MODEL AND DYNAMIC SCALING ANALYSIS

A. Model

In the absence of an external magnetic field, the Hamiltonian of the three-dimensional (3D) Ising model with a line defect on a free surface can be written as the sum of bulk interactions, surface interactions, and line interactions:

$$H = -J_b \sum_{\langle xyz \rangle} \sigma_{xyz}\sigma_{x'y'z'} - J_s \sum_{\langle xy \rangle} \sigma_{xyz}\sigma_{x'y'z} - J_l \sum_{\langle y \rangle} \sigma_{xyz}\sigma_{xy'z}, \tag{1}$$

where spin σ can take values ± 1 and $\langle \cdots \rangle$ indicates a summation over all nearest neighbors. As shown in Fig. 1(a), the last summation runs over all links on the defect lines, the second summation runs over the surface links excluding those on the defect lines, and the first summation extends over all bulk links including those with one site on the surface. J_b, J_s, and J_l are the coupling constants for the bulk, surface, and defect line, respectively. For the ferromagnetic

*Corresponding author. zheng@zimp.zju.edu.cn

 ©2008 The American Physical Society

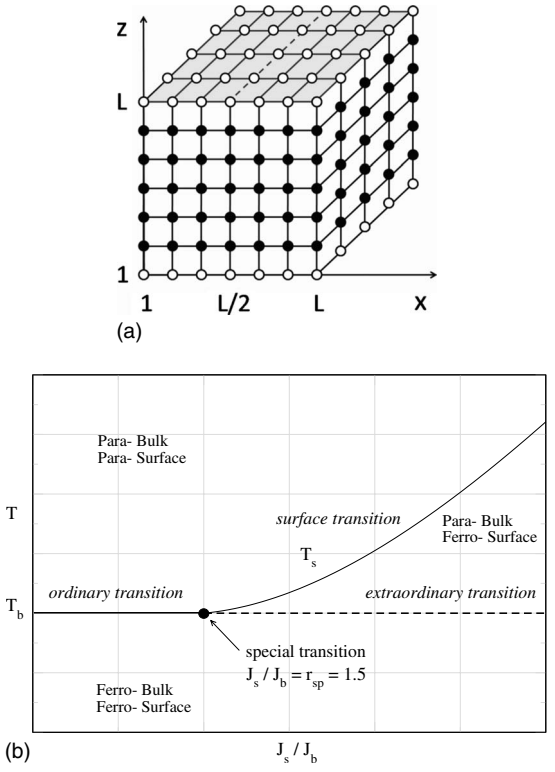

FIG. 1. (a) Schematic view of the 3D Ising model with the free surfaces at $z=1$ and L (shadowed). The defect lines at $x=L/2$ (dashed) are on the surfaces. The solid circles are spins at the bulk while the open circles are spins at the surfaces. (b) Schematic phase diagram of the semi-infinite 3D Ising model. T_b is the bulk transition temperature.

materials, J_b and J_s are positive. For convenience, we set $J_b=1.0$ in this paper.

For a perfect surface—i.e., $J_l=J_s$—it is well known that in equilibrium, there exists a special threshold r_{sp}. For $J_s<r_{sp}$, the surface undergoes a phase transition at the bulk transition temperature T_b, due to the divergent correlation length in the bulk. This phase transition is called the *ordinary* transition, and the critical behavior is *independent* of J_s. This is a *strong* universality. For $J_s>r_{sp}$, the surface first becomes ferromagnetic at the surface transition temperature $T_s>T_b$, while the bulk remains paramagnetic. If the temperature is further reduced, the bulk becomes also ferromagnetic at T_b. The former phase transition is called the *surface* transition, and the latter is called the *extraordinary* transition. This phase diagram is shown in Fig. 1(b).

It is generally believed that the surface transition belongs to the universality class of the two-dimensional (2D) Ising model [1,2]. Around r_{sp}, there occurs the crossover behavior. At exactly $J_s=r_{sp}$, the surface transition line, ordinary transition line, and extraordinary transition line meet, and the surface and bulk become critical simultaneously. This point is a multicritical point with surface exponents, and the phase transition is called the *special* transition. The best estimate of r_{sp} for the 3D Ising model in equilibrium is 1.5004(20) [39].

For an imperfect surface, generally speaking, the impact of imperfection is twofold. Let us take a surface with random-bond disorder as an example. The randomness may reduce the surface transition temperature and alter the phase diagram. For example, the special transition point of the 3D Ising model with an amorphous surface is located at $r_{sp}=1.70(1)$ [40], noticeably larger than $r_{sp}=1.5004$ for the 3D Ising model with a perfect surface. Another effect of the randomness is that it may change the universality class of the surface. The relevance or irrelevance of random imperfection on the perfect surface can be assessed by the Harris-type criterion [41].

The extended-Harris criterion states that for a surface with random-bond disorder, the disorder is relevant for $\alpha_{11}>0$, but irrelevant for $\alpha_{11}<0$, with α_{11} being the critical exponent of the surface heat capacity. Based on this criterion, the surface disorder of the 3D Ising model is irrelevant at the ordinary transition due to $\alpha_{11}<0$. Actually, this was rigorously proved by Diehl, based on the Griffiths-Kelly-Sherman inequality [42]. The situation is less clear at the special transition, for α_{11} is very close to 0. Recent simulations suggest that $\alpha_{11}<0$ and hence the disorder is irrelevant [10]. The irrelevance at the special transition has also been reported in Ref. [40]. At the surface transition, the surface is equivalent to the 2D Ising model. The disorder only leads to a logarithm correction (see Ref. [43] and reference therein).

For a surface with a defect line, the defect does *not* shift the transition temperatures of the surface transition, and therefore, the special transition point r_{sp} remains unchanged [44]. In this paper, we only consider the robustness of the ordinary, special, and surface transitions in the presence of the defect line—i.e., the possible dependence of the universality class on the coupling J_l of the defect line. In order to investigate the surface critical behavior, we apply the periodic boundary condition in the x-y plane and *free* boundary condition in the z direction, as shown in Fig. 1(a).

Let us denote the spin sitting at the site (x,y,z) by σ_{xyz}. For the perfect surface, the surface magnetization in Fig. 1(a) is defined as

$$m_1 = \frac{1}{2L^2}\sum_{xy}^{L} (\sigma_{xy1} + \sigma_{xyL}), \tag{2}$$

where L is the lattice size. For the imperfect surface, the defect line is placed at the surface position $x=L/2$, and the line magnetization in Fig. 1(a) is defined as

$$m_2 = \frac{1}{2L}\sum_{y}^{L} (\sigma_{(L/2)y1} + \sigma_{(L/2)yL}). \tag{3}$$

In this paper, with Monte Carlo simulations we study the dynamic relaxation of the 3D Ising model with perfect and imperfect surfaces starting from an ordered state. The standard Metropolis algorithm with a single-spin flip is adopted in the simulations. Therefore, the Monte Carlo dynamics belongs to the universality class of the Glauber dynamics. The numerical results are obtained with lattice sizes up to $L=128$. We measure the surface and line magnetization during the dynamic relaxation and average over 5000–20000 runs with different random numbers. Error bars are estimated by dividing the total samples into two or three subgroups and by measuring the exponents at different time intervals. Most

simulations are carried out on the Dawning 4000A supercomputer, and the total CPU time is about 3 node-year.

B. Dynamic scaling analysis

For a dynamic process, in which the system is initially in a high-temperature state, suddenly quenched to the critical temperature, and then released to the dynamic evolution of model *A*, one expects that there exist universal scaling behaviors already in the *macroscopic short-time regime* [15]. This has been shown theoretically and numerically in a variety of statistical systems [15–17,21], and it explains also the spin-glass dynamics. Furthermore, the short-time dynamic scaling behavior has been extended to the dynamic relaxation with an ordered initial state or a semiordered initial state, based on numerical simulations [17,27,35]. Recent renormalization group calculations also support the short-time dynamic scaling form for an ordered initial state [25].

On the other hand, Ritschel and Czerner have generalized the short-time critical dynamics to the magnetic system with a free surface and derived the dynamic scaling form for the dynamic relaxation with a high-temperature initial state [36]. Recent developments can be found in Refs. [37,38]. In this paper, we alternatively focus on the dynamic relaxation with an ordered initial state and with perfect and imperfect surfaces. As pointed out in the literature [17,20], the fluctuation is less severe in this case. It helps one obtain a more accurate estimate of the critical exponents at the surface. From a theoretical point of view, it is also interesting to study the dynamic relaxation with an ordered or even a more general initial state [25,27,35].

Similar to the scaling analysis at bulk [15,17,25,31,45], we phenomenologically assume that for the dynamic relaxation with an ordered initial state, the surface magnetization at a transition temperature decays by a power law

$$\langle m_1(t)\rangle \sim t^{-\beta_1/\nu_s z_s}, \tag{4}$$

which holds already in the macroscopic short-time regime, after a microscopic time scale t_{mic}. Here $\langle\cdots\rangle$ represents the statistical average, β_1 is the static exponent of the surface magnetization, ν_s is the static exponent of the spatial correlation length, and z_s is the dynamic exponent of the Glauber dynamics. For the *ordinary* and *special* transitions, where the criticality of the surface originates from the divergent correlation length in the bulk, there are no genuine new surface dynamic exponent z_s and static exponent ν_s. In other words, ν_s and z_s are just the same as those in the bulk, $\nu_s=\nu_{3D}$ and $z_s=z_{3D}$. On the other hand, β_1 is neither that of the 2D Ising model nor that of the 3D Ising model [12]. For the *surface* transition, where the critical fluctuation of the surface is of the universality class of the 2D Ising model, it is generally believed that all static and dynamic exponents are the same as those of the 2D Ising model with the Glauber dynamics [1,2]—i.e., $\beta_1=\beta_{2D}=1/8$, $\nu_s=\nu_{2D}=1$, and $z_s=z_{2D}\approx 2.16(1)$ [17].

Another important observable is the second moment of the surface magnetization, or the time-dependent surface susceptibility, defined as

TABLE I. The bulk critical temperature and critical exponents of the 3D Ising model.

T_b	ν_{3D}	z_{3D}
4.5115248(6) [52]	0.6298(5) [53]	2.042(6) [45]

$$\chi_{11} = L^{d-1}[\langle m_1^2\rangle - \langle m_1\rangle^2]. \tag{5}$$

Simple finite-size scaling analysis [17,31,45] reveals

$$\chi_{11}(t) \sim t^{\gamma_{11}/\nu_s z_s}. \tag{6}$$

Here the exponent γ_{11}/ν_s is related to β_1/ν_s by $\gamma_{11}/\nu_s=d-1-2\beta_1/\nu_s$, with $d=3$ being the spatial dimension of the bulk. This is nothing but the scaling law in equilibrium between the exponent of the surface susceptibility and that of the surface magnetization. Therefore, one can also understand the scaling behavior in Eq. (6) in an intuitive way. In equilibrium, the surface susceptibility χ_{11} of a finite lattice behaves as $\chi_{11}\sim L^{\gamma_{11}/\nu_s}$. In the dynamic evolution, $\chi_{11}(t)$ should evolve with the nonequilibrium spatial correlation length $\xi(t)$ by $\chi_{11}(t)\sim\xi(t)^{\gamma_{11}/\nu_s}$, for the finite-size effect is negligible. Then the growth law $\xi(t)\sim t^{1/z_s}$ immediately leads to Eq. (6).

Alternatively, one can construct the second cumulant $U(t)=\langle m_1^2\rangle/\langle m_1\rangle^2-1$. Obviously, $U(t)\sim t^{(\gamma_{11}+2\beta_1)/\nu_s z_s}$. From the scaling law $(\gamma_{11}+2\beta_1)=(d-1)\nu_s$, the scaling behavior of $U(t)$ then comes to the standard form [17,45],

$$U(t) \sim t^{(d-1)/z_s}, \tag{7}$$

with $d-1$ being the spatial dimension of the surface.

Equations (4), (6), and (7) above involve the bulk exponents ν_s and z_s. Therefor an accurate estimate of the surface critical exponent β_1 needs precise values of ν_{3D} and z_{3D}, as well as z_{2D}. Since the 3D Ising model at bulk has been extensively studied with various methods, many accurate results of the critical exponents and transition temperature are available. In this paper, we mainly concentrate our attention on the surface exponents and basically take the bulk exponents as input. We summarize the results of the bulk exponents of the 3D Ising model in Table I. The criteria to choose those values are their relative accuracy, as well as the methods used to extract the exponents.

From Eqs. (4) and (6), or from Eqs. (4) and (7), we obtain independent measurements of two critical exponents—e.g., β_1/ν_s and z_s. Alternatively, if we take ν_s and z_s as input, we have two independent estimates of the static exponent β_1 of the surface magnetization. This may testify to the consistency of our dynamic scaling analysis.

It is straightforward to show that the dynamic scaling forms of the line magnetization and line susceptibility have the same forms as those of the surface observables. We denote the exponents of the line magnetization and line susceptibility as β_2 and γ_{22}, respectively. The exponent γ_{22}/ν_s is related to β_2/ν_s by $\gamma_{22}/\nu_s=d-2-2\beta_2/\nu_s$, and the second cumulant behaves as $U(t)\sim t^{(d-2)/z_s}$.

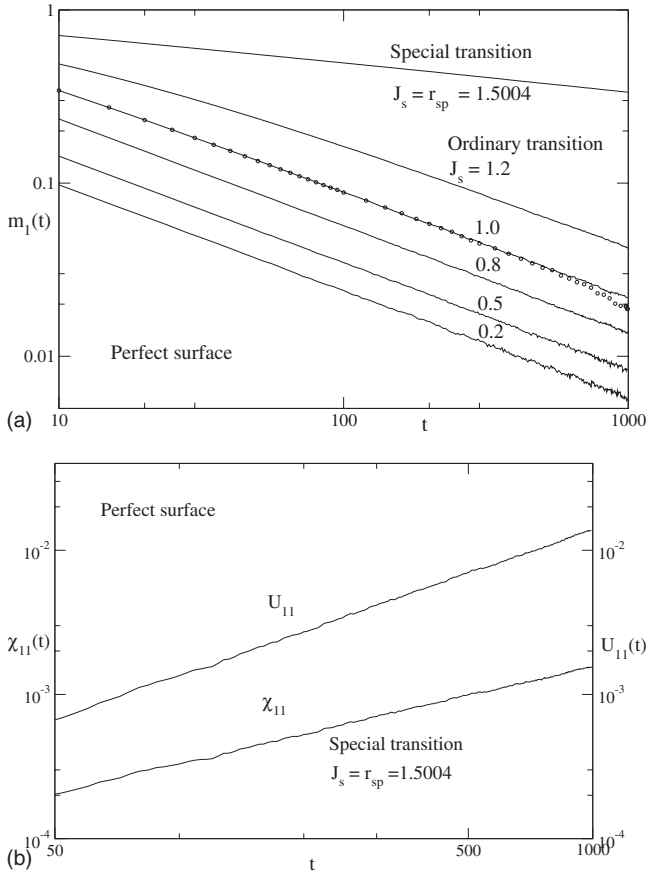

FIG. 2. (a) Dynamic relaxation of the surface magnetization at the ordinary transition with various J_s and at the special transition at $J_s=r_{sp}=1.5004$ plotted on a double-logarithmic scale. The temperature is set to the critical temperature T_b of the bulk, and the lattice size is $L=80$. Open circles are the data for $J_s=1.0$ and $L=40$. Far away from the special transition point, the slope of the curves is independent of J_s. (b) Dynamic relaxation of the surface susceptibility and second cumulant at the special transition plotted on a double-logarithmic scale. The lattice size is $L=128$.

III. SHORT-TIME DYNAMICS AT A PERFECT SURFACE

In this section we study the nonequilibrium critical dynamics at a perfect surface—i.e., $J_l=J_s$. To investigate the critical behavior of the surface, it is important to know the special transition point r_{sp}. For a perfect surface of the 3D Ising model, there exist rather accurate estimates of r_{sp} from numerical simulations in equilibrium—e.g., $r_{sp}=1.5004(20)$ in Ref. [39]. We adopt this value as the special transition point. As will be illustrated later, the special transition point r_{sp} can be also extracted from the scaling plot of a dynamic crossover scaling form.

For the ordinary phase transition, the dynamic relaxation of the surface magnetization with different J_s is shown in Fig. 2(a). Here we keep in mind that we have set $J_b=1$. The curves of $J_s=1.0$ with $L=40$ and $L=80$ overlap up to $t \geqslant 300$ MCS (Monte Carlo sweeps). It indicates that the finite-size effect is negligibly small for $L=80$ at least up to $t\sim 1200$ MCS, for the correlating time of a finite system increases by $t_L\sim L^z$. In Fig. 2(a), a power-law behavior is observed for all J_s. The microscopic time scale t_{mic}, after which the short-time universal scaling behavior emerges, or in other words, after which the correction to scaling is negligible, gradually increases as the surface coupling is being enhanced. For $J_s=0.2$, $t_{mic}\approx 10$ MCS, while for $J_s=1.2$, $t_{mic}\approx 100$ MCS.

By fitting the curves in Fig. 2(a) to Eq. (4), we obtain $\beta_1^{ord}=0.790(7)$, 0.792(6), 0.795(6), 0.786(6), and 0.755(12) for $J_s=0.2$, 0.5, 0.8, 1.0, and 1.2, respectively. The values of β_1^{ord} for $J_s=0.2$, $J_s=0.5$, and $J_s=0.8$ are consistent with each other within errors. It indicates that the ordinary transition is universal over a wide range of J_s. Deviation occurs for $J_s>1.0$ and manifests itself as the effect of the crossover to the special transition. This is in agreement with the observation in Ref. [8]. From our analysis, $\beta_1^{ord}=0.795(6)$ is a good estimate for the ordinary transition. In Table II, we compile all the existing results obtained with numerical simulations and analytical calculations in equilibrium and our measurements from the nonequilibrium dynamic relaxation. A reasonable agreement in β_1^{ord} is observed. Part of the statistical error in our measurements is from the input of the bulk exponents ν_s and z_s.

Now one may proceed to investigate the time-dependent susceptibility $\chi_{11}(t)$. In the case of the ordinary transition of the 3D Ising model, however, γ_{11} is negative. According to Eq. (6), $\chi_{11}(t)$ should decay during the time relaxation. For the ordered initial state, however, $\chi_{11}(0)=0$. Therefore, $\chi_{11}(t)$ practically fluctuates around 0 and the power-law behavior in Eq. (6) could not be observed. Nevertheless, γ_{11} is positive at the special transition, and the situation is different. The power-law behavior of the surface susceptibility and second cumulant can be detected.

In Figs. 2(a) and 2(b), the surface magnetization, surface susceptibility and second cumulant are displayed at the special transition $J_s=r_{sp}$. A power-law behavior is observed for all three observables. From the slope of the curve of the surface magnetization, we measure $\beta_1^{sp}/\nu_s z_s=0.171(2)$ and then obtain $\beta_1^{sp}=0.220(3)$ with ν_s and z_s in Table I as input. From the curve of the surface susceptibility, we measure

TABLE II. The surface critical exponents for the ordinary and special transitions of the 3D Ising model, obtained with different techniques: MF, mean-field methods; MC, Monte Carlo simulations; FT, field-theoretical methods; CI, conformal invariance. The data marked with an asterisk (⋆) are calculated with the scaling law $2\beta_1+\gamma_{11}=(d-1)\nu_s$.

	MF [1]	MC [8]	MC [9]	MC [48]	MC [10]	MC [54]	MC+CI [52]	FT [55]	This work
β_1^{ord}	1	0.78(2)	0.807(4)	0.80(1)	0.796(1)		0.798(5)	0.796	0.795(6)
β_1^{sp}	1/2	0.18(2)	0.238(2)		0.229(1)	0.237(5)		0.263	0.220(3)
γ_{11}^{sp}	1/2	0.96(9)	0.788(1)		0.802(3)*	0.785(11)*		0.734	0.823(4)

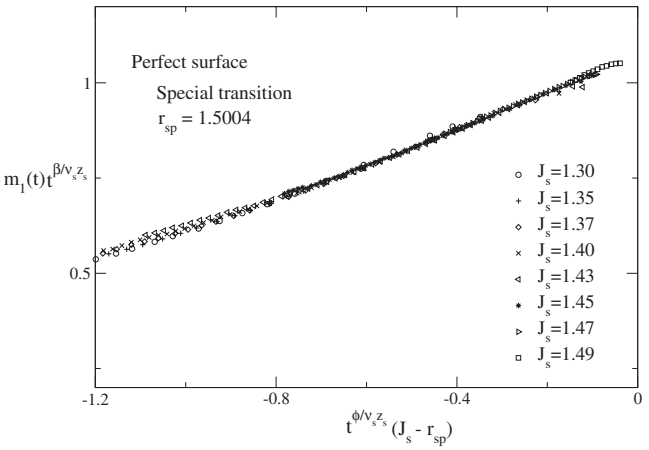

FIG. 3. Scaling plot of $m_1(t)$ according to Eq. (9) around the special transition at $J_s=r_{sp}=1.5004$. The time window in this plot is within [10, 1000]. The temperature is set to the critical temperature T_b of the bulk, and the lattice size is $L=80$.

$\gamma_{11}^{sp}/\nu_s z_s=0.640(3)$ and then calculate $\gamma_{11}^{sp}=0.823(4)$. From the scaling law $\gamma_{11}/\nu_s=d-1-2\beta_1/\nu_s$, one derives $\beta_1^{sp}=0.218(2)$, which is in good agreement with $\beta_1^{sp}=0.220(3)$ estimated from the direct measurement. The scaling behaviors in Eqs. (4) and (6) indeed hold.

The remarkable feature of the second cumulant on the surface is that its scaling behavior in Eq. (7) does not involve the exponent β_1 of the surface magnetization. From the curve in Fig. 2(b), we obtain $(d-1)/z_s=0.996(11)$ and then calculate the dynamic critical exponent $z_s=2.01(2)$. This value of z_s is very close to $z_{3D}=2.04(1)$ measured in numerical simulations in the bulk, and it confirms that the dynamic exponent on the surface is the same as that in the bulk.

In order to describe the dynamic behavior of the surface magnetization around r_{sp}, we need to introduce a crossover scaling form. To understand the crossover behavior in nonequilibrium states, we first recall the crossover scaling form in equilibrium. In equilibrium, $m_1(\tau)$ near the special transition is described by a crossover scaling form

$$m_1(\tau)\tau^{-\beta_1^{sp}}=M_{eq}(\tau^{-\phi}(J_s-r_{sp})), \tag{8}$$

where $\tau=1-T/T_b$ is the reduced temperature, ϕ is the crossover exponent, and M_{eq} is the scaling function in equilibrium. From the crossover scaling form of $m_1(\tau)$, one can determine the special transition point r_{sp} as well as β_1^{sp} and ϕ [8]. Nevertheless, up to now it has not been studied whether there also exists a corresponding crossover scaling form in nonequilibrium states. Here we will verify that such a dynamic crossover scaling form indeed exists. For simplicity, we consider the case when J_s approaches the special transition from $J_s<r_{sp}$ and the system is at the bulk critical temperature. Now the nonequilibrium spatial correlation length $\xi(t)\sim t^{1/z}$ takes the place of the equilibrium spatial correlation length $\tau^{-\nu}$. By substituting $t^{-1/\nu_s z_s}$ for τ into Eq. (8), we obtain

$$m_1(t)t^{\beta_1^{sp}/\nu_s z_s}=M_{neq}(t^{\phi/\nu_s z_s}(J_s-r_{sp})), \tag{9}$$

where M_{neq} is the scaling function in nonequilibrium. Following the ideas in Refs. [23,32,46], one should be able to determine the multicritical point r_{sp} and the exponents β_1^{sp} and ϕ from the dynamic crossover scaling form in Eq. (9). For this purpose, we perform the simulations at $J_s=1.30$, 1.35, 1.37, 1.40, 1.43, 1.45, 1.47, and 1.49 and make a scaling plot according to Eq. (9). This is demonstrated in Fig. 3. All curves of different J_s collapse into a single master curve, and it indicates that Eq. (9) *does* describe the crossover behavior during the dynamic relaxation. The scaling plot in Fig. 3 yields the exponents $\phi=0.52$ and $\beta_1^{sp}=0.220$, as well as the special transition point $r_{sp}=1.50$. The crossover exponent ϕ is very close to the mean-field value 0.5 [8], and β_1^{sp} and r_{sp} are in agreement with the existing results from the numerical simulations in equilibrium in Table II and in Ref. [39]. Although the precision of r_{sp} and critical exponents obtained here are not very high, it is still theoretically interesting. The dynamic crossover scaling form in Eq. (9) should be general, and hold in various statistical systems.

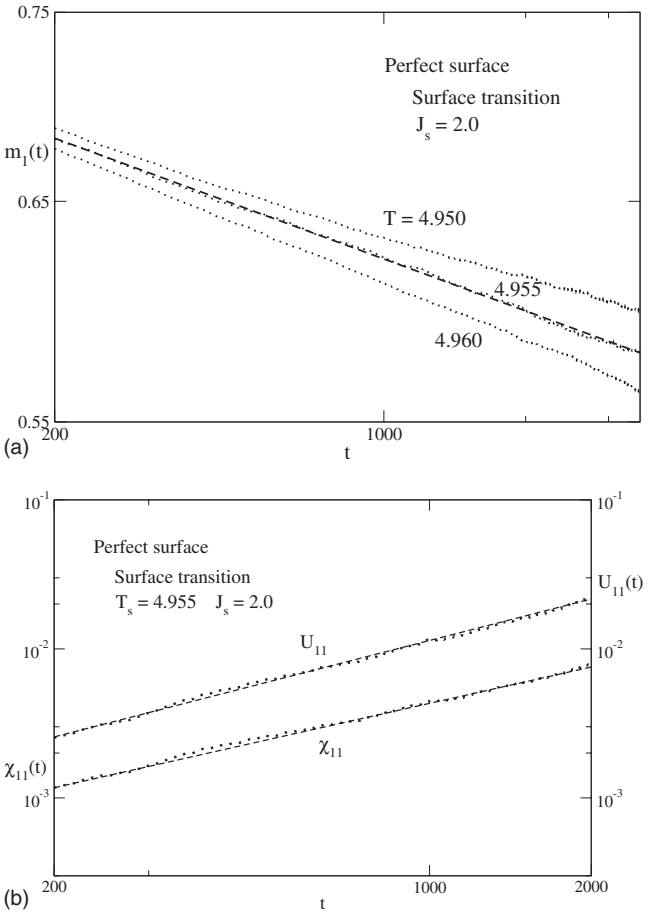

FIG. 4. (a) Determination of the surface transition temperature T_s for $J_s=2.0$. The dashed line is a power-law fit to the curve of $T=4.955$. The lattice size is $L=80$. (b) Dynamic relaxation of the surface susceptibility and second cumulant at the surface transition plotted on a double-logarithmic scale. The dashed lines are power-law fits to the curves. The lattice size is $L=80$.

To carry out the simulation at the surface transition, *we fix* J_s *at* 2.0, well above r_{sp}. At the surface transition, where the critical fluctuation is essentially two dimensional, ν_s and z_s in Eq. (4) are just ν_{2D} and z_{2D}. Around the transition temperature, the surface magnetization obeys a dynamic scaling form

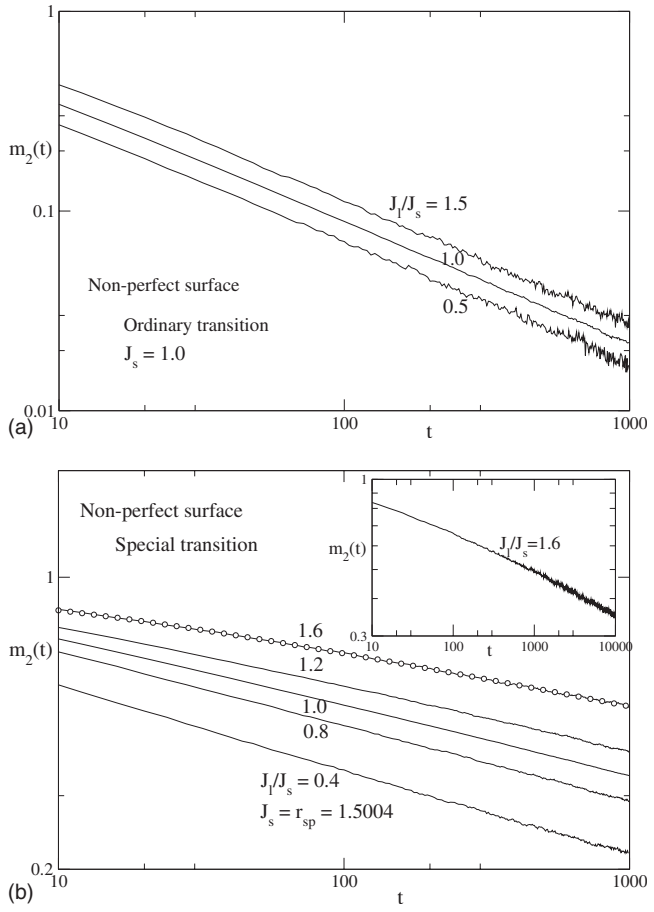

FIG. 5. (a) Dynamic relaxation of the line magnetization with various J_l plotted on a double-logarithmic scale for the ordinary transition at the imperfect surface. The slope of the curves is independent of J_l. (b) Dynamic relaxation of the line magnetization with various J_l plotted on a double-logarithmic scale for the special transition $J_s=r_{sp}=1.5004$ at the imperfect surface. The open circles show a fit according to Eq. (10) with a power-law correction to scaling. The inset displays the line magnetization at $J_l=1.6J_s$, but with a longer simulation time. The lattice size is $L=128$. The slope of the curves is dependent on J_l even after taking the correction to scaling into account.

$\langle m_1(t)\rangle \sim t^{-\beta_1/\nu_s z_s} F(t^{1/\nu_s z_s}\tau)$ [17]. To determine the surface transition temperature T_s, one may search for the curve of $\langle m_1(t)\rangle$ around T_s with the best power-law behavior; then, the corresponding temperature is identified as the transition temperature T_s. We perform the simulations with three temperatures around the transition temperature T_s and measure the surface magnetization. The results are displayed in Fig. 4(a). Interpolating the surface magnetization to other temperatures around these three temperatures, one finds the best power-law behavior of the surface magnetization at $T_s=4.955$. The corresponding slope of the curve gives $\beta_1/\nu_s z_s=0.0570(10)$ at $T_s=4.955$, and it is in agreement with the value 0.0579(3) in the 2D Ising model [17]. Therefore we take $T_s=4.955$ as the surface transition temperature, which is consistent with $T_s=4.9575(75)$ obtained with Monte Carlo simulations in equilibrium [47].

The time-dependent second cumulant U and susceptibility χ_{11} at the surface transition are measured and displayed in Fig. 4(b). The slope of the second cumulant is 0.916(15), in good agreement with $2/z_{2D}=0.926(9)$ of the 2D Ising model [17]. The slope of the susceptibility is 0.824(10), consistent with $\gamma_{2D}/z_{2D}=0.810(8)$ of the 2D Ising model. We thus confirm that the surface transition belongs to the universality class of the 2D Ising model. Meanwhile, $T_s=4.955$ is a good estimate of the surface transition temperature.

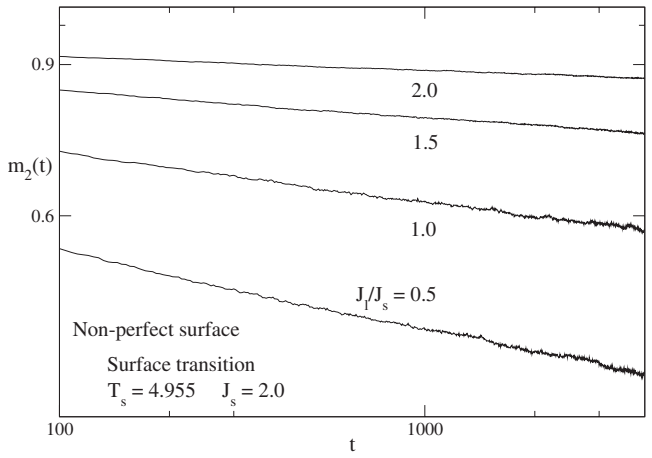

FIG. 6. Dynamic relaxation of the line magnetization with various J_l at the surface transition plotted on a double-logarithmic scale. The lattice size is $L=80$. The slopes of the curves are J_l dependent, and the results are given in Table III.

IV. SHORT-TIME DYNAMICS AT AN IMPERFECT SURFACE

In this section we investigate the nonequilibrium critical dynamics at an imperfect surface—i.e., $J_l \neq J_s$. The static and dynamic properties of an imperfect surface are important and interesting, because real surfaces are often rough, due to the impurity or limitation of experimental conditions [4]. Furthermore, the advance in nanoscience allows one to create artificial structures on top of films. We study the line defect on a surface, but the procedure can be easily generalized to other extended defects.

We first consider the dynamic behavior of the line magnetization $m_2(t)$ at the ordinary transition. For convenience, we fix $J_s=J_b=1.0$. The profiles of $m_2(t)$ with $J_l/J_s=0.5$, 1.0, and 1.5 are depicted in Fig. 5(a). All lines look parallel to each other, and it indicates that they may belong to a same universality class. By fitting these curves to the power law in Eq. (4), we estimate $\beta_2^{ord}=0.792(18)$, 0.786(6), and 0.797(33) with $J_l/J_s=1.5$, 1.0, and 0.5, respectively. These values are consistent with each other and in agreement with β_1^{ord} of the perfect surface reported in the previous section. It confirms that the defect in the ordinary transition is irrelevant in terms of the renormalization group argument. This conclusion echoes that in Ref. [40], where the impact of random bonds on the surface is investigated *in equilibrium*. The short-time dynamic approach shows its merits in identifying the universal behavior of the surface magnetization [40,47–49]. Here we note that the line magnetization is one dimensional and therefore somewhat more fluctuating than the surface magnetization.

TABLE III. Critical exponents of the defect line at the surface transition of the 2D Ising model. $\nu_s = \nu_{2D} = 1$ and $z_s = z_{2D} = 2.16(1)$ have been taken as input [17].

	Line magnetization $\beta_2/\nu_s z_s$		Susceptibility $\gamma_{22}/\nu_s z_s$		Second cumulant $1/z_s$	
Exponent	Simulation	Theory	Simulation	Theory	Simulation	Theory
$J_l = 0.5 J_s$	0.0923(36)	0.0936(9)	0.282(4)	0.276(3)	0.462(2)	0.463(4)
$J_l = 1.0 J_s$	0.0570(10)	0.0579(5)	0.356(5)	0.347(3)	0.475(2)	0.463(4)
$J_l = 1.5 J_s$	0.0301(24)	0.0307(3)	0.405(4)	0.402(4)	0.468(2)	0.463(4)
$J_l = 2.0 J_s$	0.0149(12)	0.0145(1)	0.428(9)	0.434(4)	0.459(9)	0.463(4)

Now we turn to the special transition. We perform simulations with various J_l at the special transition, and the results of the line magnetization are presented in Fig. 5(b). From the slopes of the curves, one measures the exponent $\beta_2^{sp}/\nu_s z_s$ and then calculates $\beta_2^{sp} = 0.260(4)$, 0.230(3), 0.219(5), 0.204(6), and 0.162(3) for $J_l/J_s = 0.4$, 0.8, 1.0, 1.2, and 1.6, respectively, with ν_s and z_s taken as input from Table I. Obviously β_2^{sp} changes continuously with J_l.

Since there exists a certain deviation from a power law in a shorter time for the curves with a larger ratio J_l/J_s in Fig. 5(b), one may wonder whether the variation in β_2^{sp} may stem from the correction to scaling induced by the defect line. Therefore, a careful analysis of the correction to scaling is necessary in this case. Assuming a power-law correction to scaling, $m_2(t)$ should evolve according to

$$m_2(t) = a t^{-\beta_2^{sp}/\nu_s z_s}(1 - b t^{-c}), \tag{10}$$

where a, b, and c are constants. As shown in Fig. 5(b), such an ansatz fits the numerical data well and yields $\beta_2^{sp} = 0.258(1)$, 0.235(7), 0.228(3), 0.214(6), and 0.171(3) for $J_l/J_s = 0.4$, 0.8, 1.0, 1.2, and 1.6, respectively. For $J_l/J_s = 1.6$, we extend our simulations up to a maximum time $t = 10\,000$ MCS to gain more confidence on our results. Still β_2^{sp} varies continuously with J_l, and the strong universality is violated. This is different from the case of a surface with random bonds, where the generalized Harris criterion states that the *short-range* randomness on the surface is *irrelevant* at the special transition [41]. Our result is, however, not surprising, for the defect line is not a short-range randomness [4], but an *extended* one. The defect line *does* modify the surface universality class. This can also be understood as follows. The reduction of the coupling in the defect line is somewhat like turning the local surface from the special transition to the ordinary one and therefore gives rise to a larger value of the critical exponent β_2^{sp}.

To investigate the impact of the line defect at the surface transition, we fix $J_s = 2.0$. We measure the time evolution of the line magnetization at the surface transition temperature $T_s = 4.955$ with $J_l/J_s = 0.5$, 1.0, 1.5, and 2.0, respectively. In Fig. 6, one observes that after a microscopic time $t_{mic} \approx 100$ MCS, the power-law behavior emerges. However, the exponent β_2 is J_l dependent and the strong universality is violated. This is similar to the case in Refs. [47,49], where a nonuniversal behavior of the edge and corner magnetization has been found at the surface transition.

Since the surface transition is essentially two dimensional, one may relate this imperfect surface to the 2D Ising model with a defect line. The violation of the strong universality of the 2D Ising model with a line or a ladder defect is rigorously proved by Bariev [50]. For the line defect, exact calculations show that

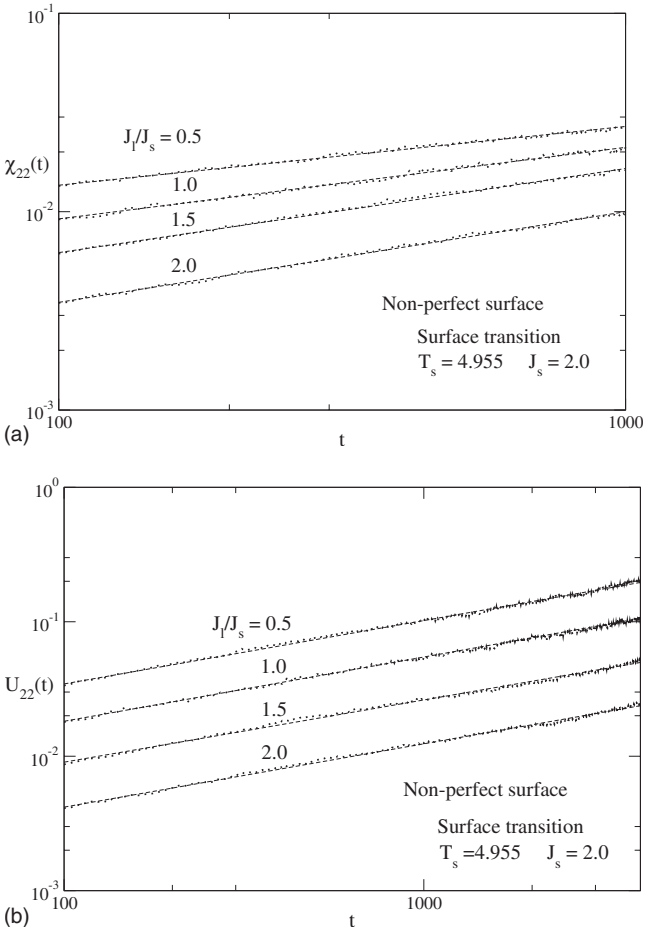

FIG. 7. (a) Dynamic relaxation of the line susceptibility with various J_l at the surface transition plotted on a double-logarithmic scale. The dashed lines are power-law fits. The slopes of the curves are J_l dependent, and the results are given in Table III. (b) Dynamic relaxation of the second cumulant of the line magnetization with various J_l at the surface transition plotted on a double-logarithmic scale. The dashed lines are power-law fits. The slopes of the curves are J_l independent, and the results are given in Table III.

$$\beta_2 = \frac{2}{\pi^2} \arctan^2(\kappa_l), \tag{11}$$

with

$$\kappa_l = \exp[-2(J_l - J)/k_B T_{2D}]. \tag{12}$$

J is the strength of the unperturbed interactions, and T_{2D} is the critical temperature of the 2D Ising model. Theoretically, the critical exponent β_2 reduces monotonically when the defect coupling J_l is enhanced. We measure the exponent β_2 and compare it with the exact values obtained from Eqs. (11) and (12). The results are summarized in Table III. One finds good agreement between the numerics and exact solution. A similar behavior of the edge magnetization, which can be viewed as a line defect at the surface transition, is also observed in Ref. [47]. Our results support the conjecture that at the surface transition, the critical exponent β_2 changes in the presence of a small perturbation.

Finally, the susceptibility $\chi_{22}(t)$ and second cumulant $U_{22}(t)$ of the line magnetization, which are similarly defined as those of the surface magnetization, are also measured. The results are plotted in Figs. 7(a) and 7(b). As stated in Sec. II, one may show that $\chi_{22}(t) \sim t^{\gamma_{22}/\nu_s z_s}$ and $U_{22}(t) \sim t^{(d-2)/z_s}$, with $\gamma_{22}/\nu_s = d - 2 - 2\beta_2/\nu_s$. The estimated exponents are also compiled in Table III, and a good consistency with the theory can be spotted.

V. CONCLUSION

With Monte Carlo simulations, we study the dynamic relaxation on perfect and imperfect surfaces of the 3D Ising model, starting from an order initial state. On the perfect surface, the dynamic behavior of the surface magnetization, susceptibility, and second cumulant is carefully analyzed at the ordinary, special, and surface transitions. The universal dynamic scaling behavior is revealed, and the static exponent β_1 of the surface magnetization, the static exponent γ_{11} of the surface susceptibility, and the dynamic exponent z_s are estimated. All the results for β_1 and γ_{11} are compiled in Table II. Since the exponents ν_s and z_s can be identified as those at the bulk, it is convenient to study different phase transitions from the nonequilibrium dynamic relaxation. Especially, the dynamic crossover scaling form in Eq. (9) is interesting. Because of the existence of the scaling variable J_s, the dynamic relaxation of the surface magnetization around the special transition does not obey a power law and the deviation from the power law is governed by the crossover exponent.

On the imperfect surface—i.e., with a defect line on the surface—the universality class of the ordinary transition remains the same as that at the perfect surface. On the other hand, at the special and surface transitions, the critical exponent β_2 of the line magnetization varies with the coupling constant J_l of the defect line. The susceptibility and second cumulant of the line magnetization also exhibit the dynamic scaling behavior and yield the static exponent γ_{22} and the dynamic exponent z_s. The short-time dynamic approach is efficient in understanding the surface critical phenomena. Furthermore, one may compare the critical dynamics at a surface with that of a domain interface [27,35,51].

ACKNOWLEDGMENTS

This work was supported in part by NNSF (China) under Grant No. 10325520. The computations are partially carried out in Shanghai Supercomputer Center.

[1] K. Binder, in *Phase Transition and Critical Phenomena*, edited by C. Domb and J. Lebowitz (Academic Press, London, 1987), Vol. 8, p. 1, and references therein.
[2] H. W. Diehl, in *Phase Transition and Critical Phenomena*, edited by C. Domb and J. Lebowitz (Academic Press, London, 1987), Vol. 10, p. 76, and references therein.
[3] H. W. Diehl, Int. J. Mod. Phys. B **11**, 3503 (1997).
[4] M. Pleimling, J. Phys. A **37**, R79 (2004).
[5] M. A. Torija, A. P. Li, X. C. Guan, E. W. Plummer, and J. Shen, Phys. Rev. Lett. **95**, 257203 (2005).
[6] K. Binder and P. C. Hohenberg, Phys. Rev. B **6**, 3461 (1972).
[7] K. Binder and D. P. Landau, Phys. Rev. Lett. **52**, 318 (1984).
[8] D. P. Landau and K. Binder, Phys. Rev. B **41**, 4633 (1990).
[9] C. Ruge and F. Wagner, Phys. Rev. B **52**, 4209 (1995).
[10] Y. Deng, H. W. J. Blöte, and M. P. Nightingale, Phys. Rev. E **72**, 016128 (2005).
[11] Y. Deng, Phys. Rev. E **73**, 056116 (2006).
[12] S. Dietrich and H. W. Diehl, Z. Phys. B: Condens. Matter **51**, 343 (1983).
[13] M. Kikuchi and Y. Okabe, Phys. Rev. Lett. **55**, 1220 (1985).
[14] H. W. Diehl, Phys. Rev. B **49**, 2846 (1994).
[15] H. K. Janssen, B. Schaub, and B. Schmittmann, Z. Phys. B: Condens. Matter **73**, 539 (1989).
[16] D. A. Huse, Phys. Rev. B **40**, 304 (1989).
[17] B. Zheng, Int. J. Mod. Phys. B **12**, 1419 (1998), review article.
[18] B. Zheng, M. Schulz, and S. Trimper, Phys. Rev. Lett. **82**, 1891 (1999).
[19] C. Godréche and J. M. Luck, J. Phys.: Condens. Matter **14**, 1589 (2002).
[20] B. Zheng, F. Ren, and H. Ren, Phys. Rev. E **68**, 046120 (2003).
[21] P. Calabrese and A. Gambassi, J. Phys. A **38**, R133 (2005).
[22] J. Q. Yin, B. Zheng, and S. Trimper, Phys. Rev. E **70**, 056134 (2004).
[23] J. Q. Yin, B. Zheng, and S. Trimper, Phys. Rev. E **72**, 036122 (2005).
[24] K. Laneri, A. F. Rozenfeld, and E. V. Albano, Phys. Rev. E **72**, 065105(R) (2005).
[25] A. A. Fedorenko and S. Trimper, Europhys. Lett. **74**, 89 (2006).
[26] E. Arashiro, J. R. Drugowich de Felicio, and U. H. E. Hansmanno, Phys. Rev. E **73**, 040902(R) (2006).
[27] N. J. Zhou and B. Zheng, Europhys. Lett. **78**, 56001 (2007).
[28] D. Stauffer, Physica A **186**, 197 (1992).

[29] N. Ito, Physica A **196**, 591 (1993).
[30] Z. B. Li, L. Schülke, and B. Zheng, Phys. Rev. Lett. **74**, 3396 (1995).
[31] H. J. Luo, L. Schülke, and B. Zheng, Phys. Rev. Lett. **81**, 180 (1998).
[32] L. Schülke and B. Zheng, Phys. Rev. E **62**, 7482 (2000).
[33] H. K. Lee and Y. Okabe, Phys. Rev. E **71**, 015102(R) (2005).
[34] X. W. Lei and B. Zheng, Phys. Rev. E **75**, 040104(R) (2007).
[35] N. J. Zhou and B. Zheng, Phys. Rev. E **77**, 051104 (2008).
[36] U. Ritschel and P. Czerner, Phys. Rev. Lett. **75**, 3882 (1995).
[37] M. Pleimling and F. Iglói, Phys. Rev. Lett. **92**, 145701 (2004).
[38] M. Pleimling and F. Iglói, Phys. Rev. B **71**, 094424 (2005).
[39] C. Ruge, S. Dunkelmann, and F. Wagner, Phys. Rev. Lett. **69**, 2465 (1992).
[40] M. Pleimling and W. Selke, Eur. Phys. J. B **1**, 385 (1998).
[41] H. W. Diehl and A. Nüsser, Z. Phys. B: Condens. Matter **79**, 69 (1990).
[42] H. W. Diehl, Eur. Phys. J. B **1**, 401 (1998).
[43] H. J. Luo, L. Schülke, and B. Zheng, Phys. Rev. E **64**, 036123 (2001).
[44] M. E. Fisher and A. E. Ferdinand, Phys. Rev. Lett. **19**, 169 (1967).
[45] A. Jaster, J. Mainville, L. Schülke, and B. Zheng, J. Phys. A **32**, 1395 (1999).
[46] J. Q. Yin, B. Zheng, V. V. Prudnikov, and S. Trimper, Eur. Phys. J. B **49**, 195 (2006).
[47] M. Pleimling and W. Selke, Phys. Rev. B **59**, 65 (1999).
[48] M. Pleimling and W. Selke, Eur. Phys. J. B **5**, 805 (1998).
[49] M. Pleimling and W. Selke, Phys. Rev. E **61**, 933 (2000).
[50] R. Z. Bariev, Sov. Phys. JETP **50**, 613 (1979).
[51] S. Z. Lin, B. Zheng, and S. Trimper, Phys. Rev. E **73**, 066106 (2006).
[52] Y. Deng and H. W. J. Blöte, Phys. Rev. E **68**, 036125 (2003).
[53] A. M. Ferrenberg and D. P. Landau, Phys. Rev. B **44**, 5081 (1991).
[54] C. Ruge, A. Dunkelmann, F. Wagner, and J. Wulf, J. Stat. Phys. **110**, 1411 (1993).
[55] H. W. Diehl and M. Shpot, Nucl. Phys. B **528**, 595 (1998).